TISSUE ENGINEERING: Part A
Volume 18, Numbers 11 and 12, 2012

DOI: 10.1089/ten.tea.2011.0614

Further Development of a Tissue Engineered Muscle Repair Construct *In Vitro* for Enhanced Functional Recovery Following Implantation *In Vivo* in a Murine Model of Volumetric Muscle Loss Injury

Benjamin T. Corona, Ph.D.,* Masood A. Machingal, Ph.D., Tracy Criswell, Ph.D., Manasi Vadhavkar, M.S., Ashley C. Dannahower, B.S., Christopher Bergman, B.S., Weixin Zhao, M.D., and George J. Christ, Ph.D.

Volumetric muscle loss (VML) can result from trauma and surgery in civilian and military populations, resulting in irrecoverable functional and cosmetic deficits that cannot be effectively treated with current therapies. Previous work evaluated a bioreactor-based tissue engineering approach in which muscle derived cells (MDCs) were seeded onto bladder acellular matrices (BAM) and mechanically preconditioned. This first generation tissue engineered muscle repair (TEMR) construct exhibited a largely differentiated cellular morphology consisting primarily of myotubes, and moreover, significantly improved functional recovery within 2 months of implantation in a murine latissimus dorsi (LD) muscle with a surgically created VML injury. The present report extends these initial observations to further document the importance of the cellular phenotype and composition of the TEMR construct *in vitro* to the functional recovery observed following implantation *in vivo*. To this end, three distinct TEMR constructs were created by seeding MDCs onto BAM as follows: (1) a short-term cellular proliferation of MDCs to generate primarily myoblasts without bioreactor preconditioning (TEMR-1SP), (2) a prolonged cellular differentiation and maturation period that included bioreactor preconditioning (TEMR-1SPD; identical to the first generation TEMR construct), and (3) similar treatment as TEMR-1SPD but with a second application of MDCs during bioreactor preconditioning (TEMR-2SPD); simulating aspects of "exercise" *in vitro*. Assessment of maximal tetanic force generation on retrieved LD muscles *in vitro* revealed that TEMR-1SP and TEMR-1SPD constructs promoted either an accelerated (i.e., 1 month) or a prolonged (i.e., 2 month postinjury) functional recovery, respectively, of similar magnitude. Meanwhile, TEMR-2SPD constructs promoted both an accelerated and prolonged functional recovery, resulting in twice the magnitude of functional recovery of either TEMR-1SP or TEMR-1SPD constructs. Histological and molecular analyses indicated that TEMR constructs mediated functional recovery via regeneration of functional muscle fibers either at the interface of the construct and the native tissue or within the BAM scaffolding independent of the native tissue. Taken together these findings are encouraging for the further development and clinical application of TEMR constructs as a VML injury treatment.

Introduction

Despite the rather well-documented capacity of skeletal muscle to repair, regenerate, and remodel following injury,[1–5] there are still a variety of traumatic injuries, and congenital and acquired diseases and disorders that result in an irrecoverable loss of muscle function. Among these is volumetric muscle loss (VML) injury, which is characterized by a degree of muscle tissue loss that exceeds the endogenous regenerative capacity of muscle resulting in permanent functional deficits of either the injured muscle or the muscle unit (i.e., in the presence of synergists).[6] VML injuries can result from trauma and surgery in both civilian and military populations and can result in devastating disablement and disfigurement.

Current treatment for VML injury involves surgical muscle transfer, although these procedures are often associated with poor engraftment and donor site morbidity (see reviews[7,8]). Physical therapy is also used to improve the strength of the VML-injured muscle or muscle unit, although

Wake Forest Institute for Regenerative Medicine, Wake Forest University Baptist Medical Center, Winston-Salem, North Carolina.
*Current affiliation: US Army Institute of Surgical Research, Fort Sam Houston, Texas.

Report Documentation Page

Form Approved
OMB No. 0704-0188

1. REPORT DATE	2. REPORT TYPE	3. DATES COVERED
01 JUN 2012	**N/A**	**-**

4. TITLE AND SUBTITLE	5a. CONTRACT NUMBER
Further Development of a Tissue Engineered Muscle Repair Construct In Vitro for Enhanced Functional Recovery Following Implantation In Vivo in a Murine Model of Volumetric Muscle Loss Injury	5b. GRANT NUMBER
	5c. PROGRAM ELEMENT NUMBER
6. AUTHOR(S)	5d. PROJECT NUMBER
Corona B. T., Machingal M. A., Criswell T., Vadhavkar M., Dannahower A. C., Bergman C., Zhao W., Christ G. J.,	5e. TASK NUMBER
	5f. WORK UNIT NUMBER
7. PERFORMING ORGANIZATION NAME(S) AND ADDRESS(ES)	8. PERFORMING ORGANIZATION REPORT NUMBER
United States Army Institute of Surgical Research, JBSA Fort Sam Houston, TX	
9. SPONSORING/MONITORING AGENCY NAME(S) AND ADDRESS(ES)	10. SPONSOR/MONITOR'S ACRONYM(S)
	11. SPONSOR/MONITOR'S REPORT NUMBER(S)

12. DISTRIBUTION/AVAILABILITY STATEMENT
Approved for public release, distribution unlimited

13. SUPPLEMENTARY NOTES

14. ABSTRACT

15. SUBJECT TERMS

16. SECURITY CLASSIFICATION OF:			17. LIMITATION OF ABSTRACT	18. NUMBER OF PAGES	19a. NAME OF RESPONSIBLE PERSON
a. REPORT	b. ABSTRACT	c. THIS PAGE			
unclassified	**unclassified**	**unclassified**	**UU**	**17**	

this treatment alone may have a limited ability to significantly restore muscle mass or function.[9] Not surprisingly, this unmet medical need has stimulated research efforts to develop new technologies for the treatment of VML injuries.

In this regard, there has been great recent interest in developing tissue engineering technologies for the treatment of VML and VML-like injuries (e.g., hernia repair).[10–18] By and large, these technologies employ either an acellular scaffold, a potentially myogenic cell source, or both, as an implantable therapeutic. For instance, injection of freshly isolated whole muscle fibers suspended in a hyaluronan-based gel was used as a means of providing satellite cells to the site of VML injury.[16] This approach resulted in improved tissue formation and functional recovery in a VML-injured mouse tibialis anterior (TA) muscle.[16] In another study, delayed injection of culture-expanded bone mesenchymal stem cells 1 week after implantation of a decellularized scaffold was also associated with restoration of muscle function in a rat gastrocnemius VML injury model.[13] Additionally, our lab has recently reported that the implantation of a differentiated tissue engineered muscle repair (TEMR) construct (i.e., comprised primarily of myotubes), which is generated following $\sim$2 weeks of static and dynamic tissue culture *in vitro*, significantly restored functional capacity while promoting new tissue formation in a VML-injured mouse latissimus dorsi (LD) muscle.[12]

As encouraging as these initial studies are, there is still significant room for therapeutic improvement. This is true with respect to both the absolute magnitude of functional recovery, and the time course of that recovery. To this end, we have begun to evaluate the ability of bioreactor-derived preconditioning protocols to modulate cellular phenotype *in vitro*, and the importance of these *in vitro* protocols to the functional recovery of VML injuries following implantation of our TEMR construct *in vivo*. The rationale for this approach is related to the supposition that the differentiation status of the muscle precursor cells used for muscle therapies can play a definitive role in the magnitude and mechanism of functional recovery. For example, under a variety of conditions including VML injury, implantation of quiescent satellite cells can promote greater regeneration compared to culture-expanded myoblasts.[16,19–21] However, while the majority of the related literature has investigated the therapeutic effects of varying degrees of maturation within relatively immature cells (i.e., quiescent vs. active satellite cells or myoblasts), very little consideration has been given to potential therapeutic differences between myoblasts and myotubes. Moreover, the advantage of employing *in vitro* tissue engineering to generate constructs comprised of a combination of myoblasts (activated satellite cells) and myotubes has not yet been explored, despite the fact that such an approach creates a scenario that recapitulates a cellular environment more akin to embryonic myogenesis and adult muscle fiber repair and hypertrophy.[22–28]

In the current study, we modified our previously reported *in vitro* tissue engineering model[12,29] to generate TEMR constructs comprised of cells resembling unfused myoblasts, myotubes, or a combination of myoblasts and myotubes. TEMR constructs were then implanted at the site of VML injury in a mouse LD muscle and functional recovery was evaluated at 1 and 2 months postinjury. The overall goal of this study was to test the hypothesis that functional recovery from VML injury can be modulated by altering the cellular phenotype and composition of the TEMR construct *in vitro* prior to implantation *in vivo*.

Methods

Experimental design

Three different strategies of culturing a mixed population of muscle derived cells (MDCs) on bladder acellular matrix (BAM) collagen scaffolds were used to create TEMR constructs with distinct morphological characteristics (Table 1). Briefly, one group of constructs was seeded primarily with MDCs and subjected to a short cellular proliferation and growth period in the absence of bioreactor preconditioning (TEMR-1SP), a second group experienced a prolonged cellular maturation period that included bioreactor preconditioning as previously described (TEMR-1SPD; see Machingal *et al.*[12]), and a third group was designed to reflect a combination of both of these conditions by applying a second population of MDCs to an underlying layer of maturing cells 3 days before implantation (TEMR-2SPD). TEMR constructs derived from all three *in vitro* protocols were implanted at the site of a surgically created VML injury in the latissimus dorsi (LD) muscle of nude mice. One and 2 months after injury and implantation, contralateral control, nonrepaired, and TEMR construct-repaired (three groups) LD muscles were retrieved. Subsequent assessments of functional capacity and tissue repair and regeneration were conducted to compare the therapeutic benefits of these distinct TEMR constructs.

Animals

Male Lewis rats (3–4 weeks) and female athymic nude/nude mice (8–10 weeks) were used as donors for MDCs or for *in vivo* studies of VML injury repair, respectively. Rodents were purchased from commercial vendors (Harlan and Jackson Laboratories). All animal procedures were approved by the Wake Forest University IACUC and are in accordance with animal use guideline set by the American Physiological Society.

MDCs isolation

Tibialis anterior and soleus muscles from 3 to 4 week old male Lewis rats were harvested for primary cell culture using methodology described previously; while the cell population isolated are identical to our previous report, herein we

Table 1. Characteristics for Creation of Tissue Engineered Muscle Repair Constructs

Construct[a]	*No. of seedings (S)*	*Proliferation media (P)*	*Differentiation media and bioreactor preconditioning (D)*
TEMR-1SP	1	Yes	No
TEMR-1SPD	1	Yes	Yes
TEMR-2SPD	2[b]	Yes	Yes

[a]Constructs are named solely by the conditions under which they were generated.

[b]Second application of MDCs occurred midway through the bioreactor preconditioning protocol.

TEMR, tissue engineered muscle repair; MDCs, muscle derived cells.

define these cells as MDCs to reflect the possibility that muscle progenitor cells among other cell types are incorporated in this cultured cell population.[12] Briefly, skeletal muscles were digested in 0.2% collagenase (Worthington biochemicals) solution prepared in low glucose Dulbecco's modified Eagle medium (DMEM; Hyclone) for 2 h at 37°C. Muscle tissue fragments were plated onto tissue culture dishes coated with Matrigel (BD Biosciences) in myogenic medium containing DMEM high glucose supplemented with 20% fetal bovine serum (FBS), 10% horse serum, 1% chicken embryo extract, and 1% antibiotic/antimycotic (Hyclone). Cells were passaged at ~75% confluence, cultured in DMEM low glucose supplemented with 15% FBS and 1% antibiotic/antimycotic, and used for seeding at the second passage.

BAM preparation

BAM scaffolds were prepared from porcine urinary bladder as previously described.[12,29] Briefly, the bladder was washed and trimmed to obtain the lamina propria, which was placed in 0.05% trypsin (Hyclone) for 1 h at 37°C. The bladder was then transferred to DMEM solution supplemented with 10% FBS and 1% antibiotic/antimycotic and kept overnight at 4°C. The preparation was then washed in a solution containing 1% triton X (Sigma-Aldrich) and 0.1% ammonium hydroxide (Fisher Scientific) in de-ionized water for 4 days at 4°C. Finally, the bladder was then washed in de-ionized water for 3 days at 4°C. The decellularized scaffold was further dissected to obtain a scaffold of 0.2–0.4 mm thickness: dimensions suitable for implantation in the surgically created mouse LD defect. The prepared acellular matrix was then cut into strips of 3 cm × 2 cm size and placed onto a custom designed seeding chamber made of silicon (McMaster Carr). Scaffolds and silicon seeding chambers were then individually placed in culture dishes and sterilized by ethylene oxide.

Preparation of TEMR constructs

As noted above, three different TEMR constructs were evaluated in these studies; TEMR-1SP, TEMR-1SPD, and TEMR-2SPD. All three TEMR constructs were created from sterilized scaffolds that were placed in custom-made silicon seeding chambers and kept immersed in a seeding media consisting of DMEM solution supplemented with 15% FBS and 1% antibiotic/antimycotic media for at least 12 h at 37°C prior to seeding. MDCs (Passage 2) were then seeded at a concentration of 1 million cells per cm^2 on one side, and after 12 h, the seeding chamber was flipped and a concentration of 1 million cells per cm^2 was seeded on the other side. After a total of 3 days in seeding media, the TEMR-1SP group was collected for either *in vitro* analyses or implantation.

The TEMR-1SPD and TEMR-2SPD constructs were subsequently immersed in differentiation media (F12 DMEM, 2% horse serum, 1% antibiotic antimyocotic [AA]) for an additional 7 days. After a total of 10 days of static culture, the TEMR-1SPD and TEMR-2SPD cell-seeded scaffolds were then placed in a bioreactor system, as described previously.[29] The bioreactor system consisted of a computer-controlled linear motor powered actuator that directed cyclic unidirectional stretch and relaxation. To permit application of the cyclic stretch protocol, one end of the TEMR construct was attached to a stationary bar, while the other end was connected to a movable bar attached to the actuator. TEMR-1SPD and TEMR-2SPD constructs were subjected to ~10% strain, three times per minute for the first 5 min of every hour, for 5–7 days (see Moon du *et al.*,[29] for details). Note that in preliminary experiments a subpopulation of TEMR-2SPD constructs also underwent three stretches times per minute for the first 5 min of every half-hour, however, this strain rate did not alter cellular morphology in any detectable fashion and we therefore considered these together as a homogeneous population of constructs for the TEMR-2SPD group. Constructs that underwent the full static and dynamic differentiation protocols as previously described[12] comprised the TEMR-1SPD group. However, the TEMR-2SPD group was created by stopping uniaxial stretching midway through preconditioning (i.e., 2–3 days), applying a second set of MDCs (first or second passage) at a density of 1 million cells per cm^2 to only one side of the construct, allowing for static cellular adherence over a 6–12 h period, and then proceeding with uniaxial stretching (same conditions) for 2 days. In all cases, during the entire cell culture process, both cell-seeded surfaces (i.e., top and bottom of the same BAM scaffold) were fully immersed in media, the constructs were continuously aerated with 95% air–5% carbondioxide (CO_2) at 37°C in an incubator, and the media were changed every 3 days.

Immunocytochemistry and analysis

MDCs (P2) were seeded either on uncoated chamber slides or BAM scaffolds at a density of 1 million cells per cm^2. Whole-mount staining was performed by fixing the cells in 2% formalin, washing in phosphate-buffered saline (PBS)-glycine (10 mM), permeabilizing with 0.5% triton, and then washing again in PBS-glycine. Cells were then blocked in 3% (w/v) nonfat dried milk in PBS for 30 min at room temperature prior to incubation with primary antibodies (1:50 in PBS) raised in mouse against desmin (Santa Cruz, 7955), MyoD (Hybridoma Bank), and Pax7 (Hybridoma Bank) or phalloidin-Alexa Fluor 488 or 594 conjugated (1:50, Invitrogen) for 1 h. After washing in PBS, cells were incubated in Texas Red-conjugated anti-mouse IgG (Vector; 1:100) secondary antibody for 30 min and were then washed again in PBS. Probed specimens were then coversliped with ProLong Gold including DAPI (Invitrogen-P36931).

To determine the percentage of P2 MDCs expressing Pax7, MyoD, or desmin on chamberslides, the total number of nuclei and positively labeled nuclei were counted in at least 12 high-powered field (400×) images from at least two different chamber slides, resulting in over 800 nuclei counted per protein marker. The percentage of positive cells is expressed as total positive cells out of total cells counted. To assess the cellular morphology and number of nuclei on BAM scaffolds, the number of nuclei and number of multinucleated cells were counted from 400× images derived from at least three different constructs from each group. The number of nuclei was counted using ImageJ software and the number of multinucleated cells was determined by a researcher who was blinded to the experimental conditions. Multinucleated cells were defined as a structure in which two or more nuclei were associated with the same set of actin stress fibers.

BAM scaffold mechanical testing

Uniaxial tensile mechanical testing was performed using an Instron 55401. Prepared sterilized BAM scaffolds were incubated at 37°C in DMEM for ~24 h prior to testing. BAM samples were uniformly prepared with a width of 3.75 mm using a standard steel press. Samples were kept hydrated during preparation and testing. Pretension was set to 0.2 N. Samples were tested to failure using a strain rate of 0.5 mm/s. Young's modulus was calculated from the slope of the linear portion of the stress–strain curve.

Surgical creation of VML injury and TEMR construct implantation

VML injury was surgically created as a critical size defect (≈50%) of the LD muscle in anesthetized (isoflurane) nu/nu mice using a previously reported methodology.[12] Briefly, a longitudinal incision was made along the midline of the back. The trapezius muscle that covers the LD muscle was lifted to expose the LD muscle without removing the tendon inserted at the humerus. Suture markers were then placed on the LD muscle demarking the superior half of the spinal fascia and the medial half of the of the muscle head at the humerus. The medial half of the muscle was then excised using a fine scissor. Using this methodology, a defect weighing ≈18 mg was excised from the LD muscle. The injured LD muscle was then either left without further treatment or an ≈3×1 cm TEMR construct was sutured (Vicryl 6-0) to the site of injury. In all cases, the fascia and skin were then sutured and closed, and the animals were allowed to recover from anesthesia. Of note, since a prior report documented that implantation of the BAM scaffold alone had no detectable effect on functional recovery, that group was excluded from consideration in the present study.[12]

In vitro *functional assessment*

Whole LD muscles were dissected free and studied *in vitro* using a DMT organ bath system (DMT Model 750TOBS) using similar methodology as described previously.[12,30–32] LD muscles were mounted in an organ bath chamber containing a Krebs-Ringer bicarbonate buffer (pH 7.4) with (in mM) 121.0 NaCl, 5.0 KCl, 0.5 $MgCl_2$, 1.8 $CaCl_2$, 24.0 $NaHCO_3$, 0.4 NaH_2PO_4, and 5.5 glucose (the buffer was equilibrated with 95% oxygen (O_2)–5% CO_2 gas). The distal tendon was attached by silk suture and cyanoacrylate adhesive to a fixed support, and the proximal tendon was attached to the lever arm of a force transducer (Dmt 750TOBS). The muscle was positioned between custom-made platinum electrodes. Direct muscle electrical stimulation (0.2 ms pulse at 30 V) was applied across the LD muscle using a Grass S88 stimulator (Grass Instruments). Real time display and recording of all force measurements were performed on a PC with Power Lab/8sp (ADInstruments).

Once the LD muscles were mounted in the organ bath, the muscles were allowed to equilibrate for 5 min prior to determining optimal physiological muscle length (L_o) via a series of twitch contractions. Maximal force as a function of stimulation frequency (1–200 Hz) was measured at 35°C during isometric contractions (750 ms trains of 0.2 ms pulses), with 2 min between contractions. Absolute forces (mN) as a function of stimulation frequency were fit with the following equation:

$$f(x) = \min + (\max - \min)/[1 + (x/EC_{50})^{-n}]. \quad (1)$$

Where x is the stimulation frequency, min and max are the smallest (i.e., twitch; P_t) and largest (i.e., peak tetanic; P_o) respective forces estimated. EC_{50} is the stimulation frequency at which half the amplitude of force (max − min) is reached and n is the coefficient describing the slope of the steep portion of the curve. Measured P_t and P_o and maximal tetanic force at 80 Hz (P_{80Hz}), an index of measured force at approximately EC_{50}, were compared during statistical analyses.

Additionally, P_o was normalized to an approximate physiological cross-sectional area (PCSA), which was calculated using the following equation:

$$\text{PCSA} = \{\text{wet wt.(g)}/[\text{muscle density (g/cm}^3) \times (\text{muscle length(cm)})]\}. \quad (2)$$

Where muscle density is 1.06 g/cm^3.[33–35]

For a subset of muscles, following force–frequency testing a caffeine contracture force assessment was performed using similar methodology described previously.[12,31,32] For these studies, a maximal caffeine contracture response was elicited by exposing the muscle to 50 mM caffeine during twitch contractions at a rate of 0.2 Hz.[31] This concentration of caffeine was chosen because concentrations in the mM range have been previously shown to maximally stimulate whole uninjured and injured rodent skeletal muscle.[31,36,37] During this testing, resting tension of the muscle increases until active force and resting tension are indistinguishable and then the response plateaus. Peak caffeine contracture force was defined as the tension measured at this steady-state response.

Western blotting

TEMR constructs collected before implantation were rinsed with PBS and then minced and incubated for 30 min in 200 μL of NP-40 lysis buffer with a protease inhibitor cocktail (PIC: 40 μL/mL; Sigma P8340) resting on ice. Following incubation, the lysis suspension was centrifuged at 7000 *g* for 10 min at 4°C. The supernatant was stored at −80°C until further use.

Uninjured, injured, and injured and repaired whole LD muscles were snap frozen in liquid nitrogen and stored at −80°C. LD muscles were thawed on ice, minced in 800 μL of homogenization buffer A (250 mM sucrose, 100 mM KCl, 20 mM MOPS, and 5 mM EDTA, pH 6.8) + PIC, and then homogenized using a PowerGen 125 tissue homogenizer (Fisher Scientific) to make a whole muscle homogenate. A portion (675 μL) of the whole homogenate was then further processed to extract the myofibrillar fraction. Whole homogenates were centrifuged at 10,000 *g* for 10 min at 4°C. The pellet was then resuspended in a 800 μL of wash buffer (175 mM KCl, 2 mM EDTA, 0.5% triton X 100, and 20 mM MOPS, pH 6.8) prior to undergoing a second centrifugation at 10,000 *g* for 10 min at 4°C. The pellet was then resuspended in 500 μL of homogenization buffer C (150 mM KCl and 20 mM MOPS, pH 7.0) with protease inhibitor

cocktail. Whole muscle and myofibrillar fraction homogenates were stored at 80°C until use. Protein concentration in homogenates was determined using a Bradford assay (Biorad Protein Assay Dye Reagent – 500-0006).

TEMR construct, whole muscle, and myofibrillar homogenates were diluted in laemmli sample buffer with β-mercaptoethanol and then placed in boiling water for 3 min. From each respective homogenate type 60, 25, and 15 μg of protein per sample was loaded into 7%, 7%, and 10% polyacrylamide gels and separated using sodium dodecyl sulfate polyacrylamide gel electrophoresis (SDS-PAGE). The separated proteins were then transferred to a polyvinylidene fluoride membrane (Millipore, Immobolin 0.45 μm pore), which was blocked overnight at 4°C in 5% (w/v) nonfat dried milk suspended in PBS-Tween. For the TEMR construct protein expression characterization, membranes were probed with mouse-derived anti-desmin (Sigma D1033; 1:200), Pax7 (Hybridoma Bank; 1:25), myosin (Hybridoma Bank MF20; 1:100), embryonic myosin heavy chain (MHC_{emb}; Hybridoma Bank F1.652; 1:100), and GAPDH (Millipore MAB374; 1:1000) in PBS-T for 3 h at room temperature. For the whole LD muscle homogenate analysis, membranes were probed with rabbit-derived anti-junctophilin1 (Invitrogen 40-5100; 1:20,000) and mouse-derived anti-desmin (Sigma D1033; 1:200), Pax7 (Hybridoma Bank; 1:50), and GAPDH (Millipore MAB374; 1:1000) in PBS-T for 2 h at room temperature. For the myofibrillar fraction homogenate analysis, membranes were probed with mouse-derived anti-myosin (Hybridoma Bank MF20; 1:500) and GAPDH (Millipore MAB374; 1:1000). After washing in PBS-T, membranes were incubated in anti-mouse or rabbit HRP conjugated secondary antibodies (Cell Signal 7074 and 7076) in PBS-T (1:20,000) for 2 h at room temperature. Membranes were washed in PBS-T before detection using a SuperSignal West Femto Chemiluminescent Substrate kit (Thermo Scientific 34096) and Fujifilm Intelligent Dark Box (LAS-3000). Optical density of the blot was determined using ImageJ. All protein markers were normalized to the optical density of GAPDH.

Histology and immunohistochemistry

LD muscles from all experimental groups were fixed in 10% neutral buffered formalin and stored in 60% ethanol. All samples were processed (ASP300S, Leica Microsystems) and then embedded in paraffin (EG1160, Leica Microsystems). Seven micrometer thick serial sections were cut from the paraffin embedded blocks and Masson's trichrome staining and immunohistochemical staining was performed using standard procedures. Immunohistochemical staining was performed using antibodies to detect desmin (M0760, 1:75, Dako), junctophilin 1 (Jp1; Invitrogen 40-5100, 1:120), myosin (MF-20, 1:10), ryanodine receptor 1 (RyR1; 34C, 1:10), and Pax7 (1:150). MF-20, RyR1, and Pax7 antibodies were acquired from Developmental Studies Hybridoma Bank, Iowa City, IA. Biotinylated anti-mouse IgG (MKB-2225, 1:250, Vector Laboratories Inc.) and anti-rabbit (BA-1000, 1:500, Vector Laboratories Inc.) secondary antibodies were used to detect mouse (desmin, MF-20, RyR1, and Pax7) and rabbit (Jp1) primary antibodies. The sections were next treated with Avidin Biotin Complex Reagent (PK-7100, Vector Laboratories Inc.) and then visualized using a NovaRED substrate kit (SK-4800, Vector Laboratories Inc.). Finally, the sections were counterstained using Gill's Hematoxylin (GHS280, Sigma-Aldrich). Tissue sections without primary antibody were used as negative controls. Images were captured and digitized (DM4000B Leica Upright Microscope, Leica Microsystems) at varying magnifications.

Statistics

Dependent variables were separately analyzed with one-way analysis of variance (ANOVA). Upon finding a significant ANOVA ($p < 0.05$), *post-hoc* analysis was performed using independent samples *t*-tests with Fisher's least significant difference (LSD) correction. Statistical significance was set at an $\alpha < 0.05$. Statistical analyses were performed using SPSS 18.0.

Results

BAM characterization

BAM scaffolds were prepared and seeded with MDCs as described previously.[12] Examination of decellularized BAM scaffolds confirmed the absence of nuclei or cellular protein (Fig. 1). Tensile mechanical properties of BAM scaffolds prior to seeding with MDCs were also characterized. BAM scaffolds exhibited a Young's Modulus of 7.6 ± 1.3 MPa with a stress of 1.1 ± 0.2 MPa at failure, which are similar to values previously described for acellular collagen matrices.[38]

MDC characterization

P2 cells were seeded on glass chamber slides with no coating, and incubated for 1 day in proliferation media (DMEM; 15% FBS; 1% AA). At this time and under these conditions, the percentage of cells expressing Pax7, MyoD, and desmin was ~36%, 34%, and 21% respectively (Fig. 1); reflecting the relative heterogeneity of the cell population.

TEMR construct characterization prior to implantation

As noted in the Methods section and summarized in Table 1, three distinct TEMR constructs were produced. All constructs were initially seeded with MDCs (denoted as 1S—first seeding) and placed in proliferation media (denoted as P). One of the TEMR constructs was implanted immediately after proliferation and prior to bioreactor preconditioning (denoted as the TEMR-1SP). The other two construct types were placed in differentiation media (denoted as D) and subjected to bioreactor preconditioning prior to implantation. However, one of those constructs received a second seeding of MDCs (denoted by the 2S for a second round of seeding) midway through the bioreactor preconditioning protocol (TEMR-2SPD) while the other did not (TEMR-1SPD); again, see Table 1 and Methods section for additional details concerning the nomenclature and culture conditions. As illustrated in Fig. 2 the three TEMR constructs exhibited distinct morphological characteristics (Fig. 2). In particular, for the TEMR-1SP constructs, the cells were largely unfused and not aligned (Fig. 2A). For the TEMR-1SPD and TEMR-2SPD constructs (differentiation medium + uniaxial mechanical strain) the cells exhibited an elongated and aligned morphology. The total number of nuclei was significantly reduced following bioreactor preconditioning for TEMR-1SPD constructs. However, the addition of a second batch of MDCs to an underlying layer of differentiating cells (i.e.,

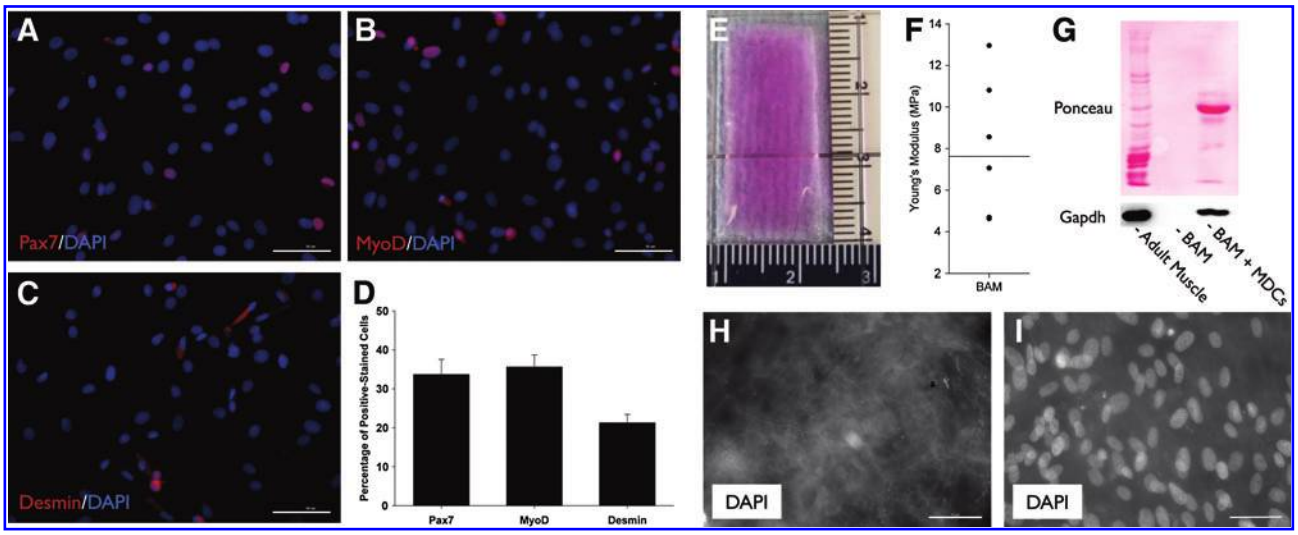

FIG. 1. Rat muscle derived cell (MDC) protein expression and bladder acellular matrix (BAM) scaffold characteristics. MDCs from primary culture were passaged once, seeded on noncoated chamber slides, and then cultured for 1 day in proliferation media (See Methods). Per protein marker **(A–C)**, the total number of nuclei and positively stained nuclei were counted in at least 12 high-powered field (400×) images from at least two different chamber slides. Over 800 nuclei were counted for each protein marker with the number of positive cells expressed as percentage of total nuclei **(D)**. BAM collagen scaffolds were cut to ~3×1 sheet prior to implantation (**E**; scaffold was rehydrated in Dulbecco's Modified Eagle Medium for picture contrast). Young's modulus was determined for seven sterilized and rehydrated scaffolds **(F)**. Scaffolds were confirmed to be decellularized via the absence of a protein (Ponceau) or specifically glyceraldehyde 3-phosphate Dehydrogenase (GAPDH) [blot; **(G)**], and the absence of nuclei [DAPI; **(H)**]. Protein expression (G) and nuclear staining via DAPI is demonstrated on BAM scaffold following the addition of MDCs **(I)**. Scale bar = 50 μm for all images. Color images available online at www.liebertonline.com/tea

TEMR-2SPD) was associated with a significant increase in the total number of nuclei on the scaffold. Moreover, the number of multinucleated cells was significantly greater for TEMR-1SPD and TEMR-2SPD compared with TEMR-1SP, with TEMR-2SPD exhibiting the greatest number of multinucleated cells (Fig. 2G).

Characterization of muscle proteins in all three TEMR constructs prior to implantation revealed expression of both immature and mature muscle markers, suggesting that each construct type is comprised of cells under multiple states of differentiation and maturation. All constructs expressed similar Pax7 and desmin protein expression relative to GAPDH (Fig. 2I). However, TEMR-1SP constructs had significantly greater levels of myosin than TEMR-1SPD constructs, and significantly greater levels of embryonic MHC_{emb} than both the TEMR-1SPD and TEMR-2SPD constructs.

In vitro *isometric strength analysis*

In vitro isometric force–frequency testing was conducted on whole LD muscle retrieved from a total of five experimental groups [i.e., native control (uninjured); VML injured but not repaired (NR); and TEMR-1SP, TEMR-1SPD, and TEMR-2SPD repaired] at either 1 or 2 months postimplantation. As outlined in detail below, functional recovery was dependent on both the type of TEMR construct implanted, and the time postimplantation.

Functional recovery in the absence of TEMR implantation (no repair)

For NR muscles, peak isometric twitch force (P_t), maximal isometric force at 80 Hz stimulation (P_{80Hz}), and peak tetanic force (P_o) were significantly reduced by ~66%, 71%, and 75% compared with uninjured values 1 month postinjury (Fig. 3; Table 1). At 2 months postinjury, the NR group exhibited similar functional deficits for P_t and P_{80Hz} (~77% and 75%, respectively). Although some recovery of P_o from 1 to 2 months postinjury was observed for NR muscles (Fig. 3; Table 1), a sustained ~67% functional deficit of P_o 2 months postinjury indicates that a critical size defect was achieved in this study using this VML injury model.

Functional recovery 1 month postimplantation of TEMR constructs

At 1 month postinjury, TEMR-1SP and TEMR-2SPD constructs both exhibited improved LD function/contractility compared to NR values. More specifically, at this time P_t, P_{80Hz}, and P_o were greater than the corresponding NR values by ~96%, 106%, and 111%, for the TEMR-1SP constructs, and by ~50% ($p = 0.276$), 128%, and 120% for TEMR-2SPD constructs. In contrast, as previously reported,[12] there was little functional improvement at the 1 month time point following implantation of the TEMR-1SPD construct. That is, P_t, P_{80Hz}, and P_o values of the TEMR-1SPD construct group were not significantly different from NR (Fig. 3; Table 1). Moreover, at this time the TEMR-1SP and TEMR-2SPD groups had indistinguishable P_o values (Fig. 3; Table 1) that were ≈ 40% greater than the corresponding P_o value for the TEMR-1SPD group. Lastly, NR, TEMR-1SPD, and TEMR-2SPD treatment groups displayed a leftward shift in the force–frequency curve (i.e., EC_{50} < Uninjured; Table 2), while the TEMR-1SP group was similar to uninjured muscle value.

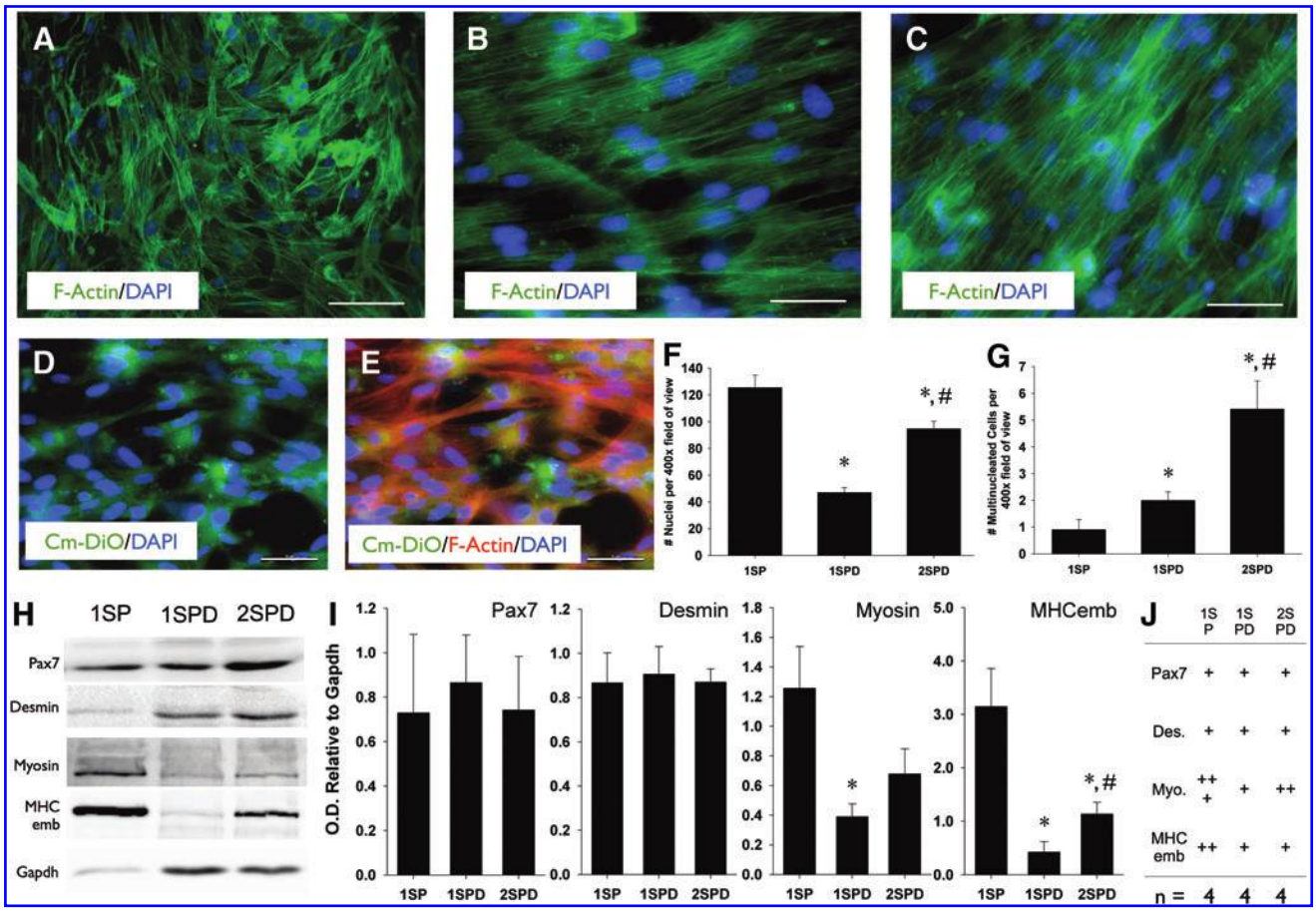

FIG. 2. Cellular morphology and protein expression characteristics of BAM-supported tissue engineered muscle repair (TEMR) constructs developed under three distinct culture conditions. TEMR-1SP, TEMR-1SPD, and TEMR-2SPD constructs are depicted in **(A)**, **(B)**, and **(C)**, respectively (400× images). For the generation of the TEMR-2SPD constructs, a second batch of MDCs was added to an underlying layer of MDCs (i.e., TEMR-1SPD constructs). To confirm adherence of the second MDC batch, these cells were loaded with cytoplasmic fluorescent dye and then visualized following preconditioning **(D** and **E)**. Scale bar = 50 μm for all images. The number of nuclei **(F)** and the number of multinucleated cells **(G)** were quantitated for each construct type (See Methods, *TEMR-1SP; #TEMR-1SPD, $p < 0.05$). Muscle-specific protein expression of TEMR constructs was characterized via Western blot **(H)**. The optical densities of specified proteins were normalized to that of GAPDH for statistical comparisons among groups [**(I)**; *significantly different from TEMR-1SP, $p < 0.05$]. Protein expression of each construct type is summarized **(J)**. Color images available online at www.liebertonline.com/tea

Functional recovery 2 months postimplantation of TEMR constructs

At 2 months postimplantation, all TEMR construct groups had significantly greater P_{80Hz} and P_o values than that observed for the NR group. However, only the TEMR-2SPD constructs produced significantly greater P_t than the NR group (Fig. 3; Table 1). The magnitude of functional recovery was also TEMR construct dependent, as noted by the fact that the P_o value of the TEMR-1SP, TEMR-1SPD, and TEMR-2SPD groups was ~60%, 62%, and 110% greater than NR at 2 months, with the TEMR-2SPD group value also significantly greater than both the TEMR-1SP and TEMR-1SPD groups. Additionally, the time course of functional recovery was also TEMR construct dependent. That is, from 1 to 2 months, the TEMR-1SPD and TEMR-2SPD construct groups exhibited a ~39% and 28% improvement in P_o, respectively, while the TEMR-1SP group showed no significant improvement (i.e., 0.2%) over this same time frame. Lastly, the leftward shift in the force–frequency curves observed at 1 month postinjury for NR, TEMR-1SPD, and TEMR-2SPD groups was rectified at 2 months.

Absolute forces were also normalized to the estimated physiological cross-sectional area to calculate specific force (N cm^{-2}). There were no significant differences among experimental groups at either 1 or 2 months postinjury and all experimental groups produced significantly less specific P_o than uninjured muscles (Table 1). LD muscle wet weight was consistently greater for all TEMR construct groups at 1 and 2 months postinjury compared with uninjured and NR groups, while LD muscle length was similar among all groups.

For a subset of muscles, peak caffeine contracture force was measured 2 months postinjury. All experimental groups were significantly reduced compared to uninjured controls (Table 1). However, all TEMR construct groups produced contracture forces similar to each other and greater contracture force than the NR group. Specifically, TEMR-1SP, TEMR-1SPD, and TEMR-2SPD treatment groups produced ~103%, 63%, and 110% greater contracture force than NR, respectively.

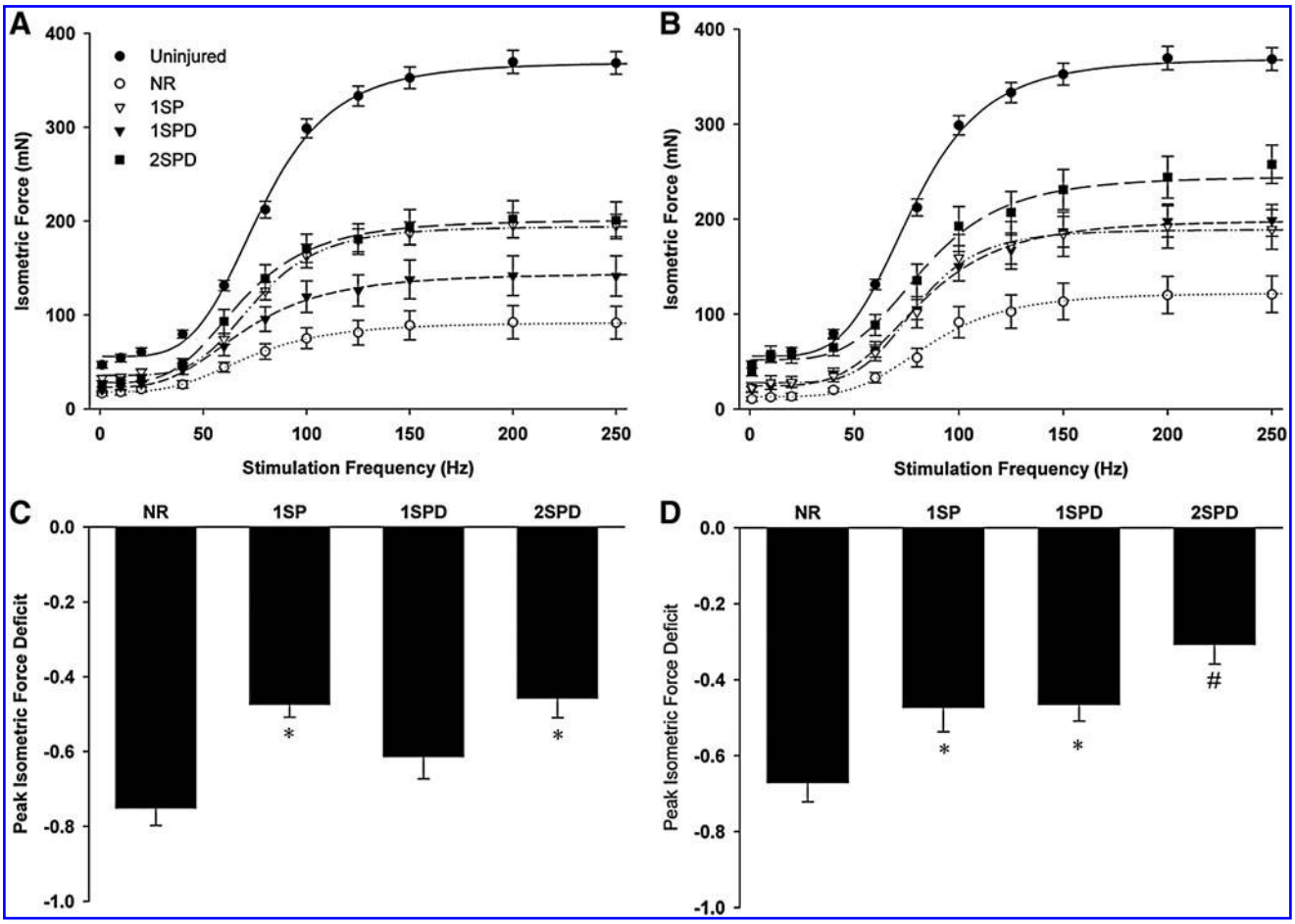

FIG. 3. Latissimus dorsi (LD) muscle *in vitro* isometric force recovery following volumetric muscle loss (VML) injury is dependent on TEMR construct type. Uninjured and injured but nonrepaired (NR) or TEMR construct (three types, TEMR-1SP, TEMR-1SPD, and TEMR-2SPD)-repaired LD muscles were tested using direct muscle stimulation at 35°C in an organ bath (See Methods). Isometric force as a function of stimulation frequency was assessed for all experimental conditions at either 1 month **(A)** or 2 months **(B)** postinjury. Force–frequency curves were fit with a Hill equation as described in the Methods section. Peak isometric tetanic force functional deficits relative to the uninjured group mean was calculated for all experimental groups at 1 month **(C)** and 2 months **(D)**. For each postinjury time, *to NR while #to all other groups ($p < 0.05$). Values are expressed as means ± standard error (SE). Sample sizes for each group at each postinjury time are listed in Table 1.

Cell- and tissue morphology

Cell- and tissue morphology of VML-injured LD muscles with and without TEMR construct repair were qualitatively characterized. Specifically, the area of VML injury where the implanted TEMR constructs interface with the remaining tissue was of particular interest and is illustrated in Fig. 4 for NR and TEMR construct repair groups at 1 and 2 months postinjury. In agreement with the observed functional deficits, the NR group exhibited gross tissue disruption, marked by the presence of small muscle fibers, increased collagen deposition, and mononuclear cells, consistent with a continued immune response at 1 month postinjury. Two months postinjury, the NR muscle appears to have completed the innate degenerative and regenerative response to the VML injury. At this time, the NR tissue shows little mononuclear cellular presence, improved muscle fiber organization, and collagen and adipose deposition at the site of injury.

Of note, in all cases, TEMR construct implantation resulted in improved tissue morphology compared with NR muscles. At 1 and 2 months postinjury the muscle fibers at the initial site of injury present qualitatively fewer signs of damage, disruption, and mononuclear cellular presence in TEMR construct-repaired versus NR tissue (Fig. 4). There were, however, distinct differences in tissue morphology among the TEMR construct groups. For example, while the muscle fibers at the interface were either regenerated or repaired by 1 month postinjury for the TEMR-1SP group, the remaining BAM scaffold was mostly devoid of a cellular presence (Fig. 4B). A similar morphology was also observed for this group at 2 months postinjury (Fig. 4F). In contrast, a cellular presence within the scaffold was observed in both the TEMR-1SPD and TEMR-2SPD construct groups. And, from 1 to 2 months there appeared to be an increase in muscle tissue formation both at the site of injury (Fig. 4C, G) and within the scaffold that was independent of the primary muscle tissue (i.e., new muscle tissue formation; Fig. 4D, H). Lastly, we also observed a marked vascular and neural presence[12] at the tissue-scaffold interface 1 month postinjury when TEMR constructs were implanted; however, there was no obvious difference in the occurrence of these structures among construct types (Fig. 5). As illustrated, the neural and

Table 2. Latissimus Dorsi Muscle Morphological Characteristics and *In Vitro* Isometric Force Parameters

		1 month postinjury				*2 months postinjury*				
	Uninjured	*NR*	*TEMR-1SP*	*TEMR-1SPD*	*TEMR-2SPD*	*NR*	*TEMR-1SP*	*TEMR-1SPD*	*TEMR-2SPD*	*Analysis of variance (p)*
Sample size	22	5	6	7	8	4	6	7	8	
Muscle characteristics										
Wet weight (mg)	90.3 ± 3.7	102.4 ± 11.8	166.1 ± 10.1[a,b]	154.8 ± 14.1[a,b]	162.0 ± 14.6[a,b]	86.6 ± 11.5	152.0 ± 14.3[a,b]	151.6 ± 23.5[a,b]	152.8 ± 17.0[a,b]	< 0.001
L_o (mm)	34.9 ± 0.8	33.3 ± 1.7	33.8 ± 1.4	36.2 ± 1.5	34.9 ± 1.4	32.6 ± 0.8	31.0 ± 2.2	31.9 ± 1.3	32.1 ± 0.6	0.099
Isometric force parameters										
$P_{t\ meas}$, mN	46.8 ± 3.5	16.1 ± 2.6[a]	31.6 ± 2.7[a,b]	19.8 ± 3.2[a]	24.1 ± 5.4[a]	10.6 ± 2.4[a]	21.9 ± 4.9[a]	20.0 ± 2.9[a]	39.0 ± 4.3[b,e]	< 0.001
$P_{80Hz\ meas}$, mN	212.2 ± 8.9	61.0 ± 8.3[a]	125.5 ± 9.6[a,b]	95.6 ± 13.2[a]	138.8 ± 14.6[a,b]	54.2 ± 9.9[a]	102.0 ± 16.4[a,b]	104.9 ± 10.7[a,b]	135.5 ± 17.1[a,b]	< 0.001
$P_{o\ meas}$, mN	374.4 ± 12.1	93.1 ± 17.3[a]	196.9 ± 13.0[a,b]	144.4 ± 21.9[a]	203.2 ± 19.7[a,b,d]	123.3 ± 19.1[a,e]	197.2 ± 24.0[a,b]	200.1 ± 16.3[a,b,e]	259.3 ± 19.3[a,b,c,d,e]	< 0.001
EC_{50}, Hz	78.7 ± 1.6	68.7 ± 4.4[a]	76.2 ± 3.6	68.4 ± 4.4[a]	68.5 ± 3.6[a]	87.0 ± 3.3[e]	81.9 ± 2.3	81.8 ± 1.5[e]	85.3 ± 4.2[e]	< 0.001
n Coefficient	4.1 ± 0.2	3.6 ± 0.2	4.6 ± 0.6	3.6 ± 0.4	4.4 ± 0.5	4.4 ± 0.3	6.1 ± 1.4	4.2 ± 0.5	4.5 ± 0.3	0.127
Specific $P_{o\ meas}$, N cm^2	15.6 ± 0.7	3.2 ± 0.5[a]	4.2 ± 0.2[a]	3.4 ± 0.7[a]	4.9 ± 0.7[a]	5.1 ± 1.0[a]	4.5 ± 0.8[a]	4.7 ± 0.3[a]	6.4 ± 1.0[a]	< 0.001
Caffeine, mN	112.5 ± 6.3	–	–	–	–	41.3 ± 3.7[a]	83.7 ± 10.8[a,b]	67.3 ± 5.4[a,b]	86.6 ± 5.5[a,b]	< 0.001

Values are mean ± standard error. LD muscle sample sizes are for measured electrical stimulation force parameters. L_o is the optimal muscle length coinciding with peak twitch force. Measured isometric twitch (P_t), titanic force at 80 Hz (P_{80Hz}), and peak titanic (P_o) force were elicted using direct electrical stimulation (0.2 ms pulse width; 30 V). EC_{50} is the stimulation frequency at which half of the rise in amplitude of force occurred. The *n* coefficient is the slope of the linear portion of the force–frequency curves depicted in Fig. 3. Absolute P_o was normalized by physiological cross-sectional area to determine specific force. Following force–frequency testing a subset of muscles performed an isometric caffeine (50 mM) contracture test. Denotations indicate statistically significantly different group means ($p < 0.05$): [a]Uninjured; [b]not repaired at same postinjury time; [c]TEMR-1SP at same postinjury time; [d]TEMR-1SPD at same postinjury time; [e]1 month for same experimental group.

LD, latissimus dorsi.

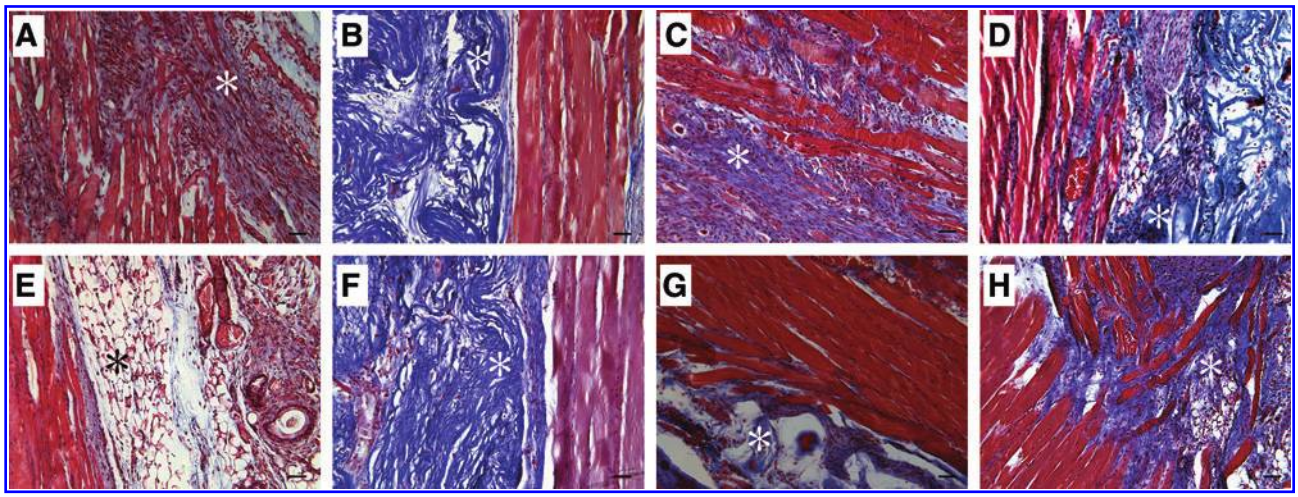

FIG. 4. LD muscle tissue morphology after VML injury and immediate repair with TEMR constructs. VML-injured LD muscles that were either not repaired **[(A)** and **(E)]** or repaired with TEMR-1SP **[(B)** and **(F)]**, TEMR-1SPD **[(C)** and **(G)]**, or TEMR-2SPD **[(D)** and **(H)]** TEMR constructs were retrieved 1 month **(A–D)** and 2 months **(E–H)** postinjury and stained using Masson's trichrome (Red = tissue, Blue = Collagen, and Black = Nuclei). *Marker of area of initial injury **[(A)** and **(E)]** or presumptive BAM collagen deposition **[(B–D)** and **(F–H)]**. Images are 200× magnification with the scale bar = 50 μm. Color images available online at www.liebertonline.com/tea

vascular structures were associated with regenerating muscle fibers in most cases.

Functional protein expression

To determine whether regenerating or newly formed muscles fibers were capable of contributing to functional recovery, TEMR construct-repaired LD muscles retrieved 2 months postinjury were stained using IHC for a host of key proteins required for force production and transmission. Two areas of interest within the repaired LD muscles were identified for investigation: (1) the area of initial VML injury at the interface between TEMR constructs and the remaining native tissue (Fig. 6A–E) and (2) at sites of tissue formation within BAM scaffolding independent from the interface (Fig. 6F–J). For all construct groups, muscle fibers in both these areas stained positively (determined by negative control and striated appearance) for desmin, myosin, ryanodine receptor 1 (RyR1), and junctophilin 1 (JP1).

To further evaluate the characteristics of TEMR-mediated functional recovery of VML injury, we quantified the relative content of specific muscle proteins involved in force production and transmission. The rationale for this approach is that the content of muscle specific contractile proteins can be reduced in injured muscle leading to functional deficits.[30,39,40] Moreover, aberrant regeneration in which crucial functional proteins are not expressed appropriately could reduce the functional recovery mediated via TEMR construct implantation. Relative protein content of desmin, JP1, and myosin (normalized to GAPDH) was quantified in whole or myofibrillar (myosin only) protein homogenates from uninjured and VML-injured LD muscles 2 months postinjury (Fig. 7). No differences among uninjured, NR, and TEMR construct groups were observed for either desmin or myosin. In comparison to all other treatment groups, JP1 was elevated for TEMR-1SP constructs ($p < 0.05$).

Pax7 expression in TEMR construct-repaired LD muscle

Lastly, while the muscle fibers at the interface appear to have completed or nearly completed the regenerative response 2 months after injury (Figs. 4 and 6) in TEMR construct-repaired LD muscles, fibers localized to the scaffold

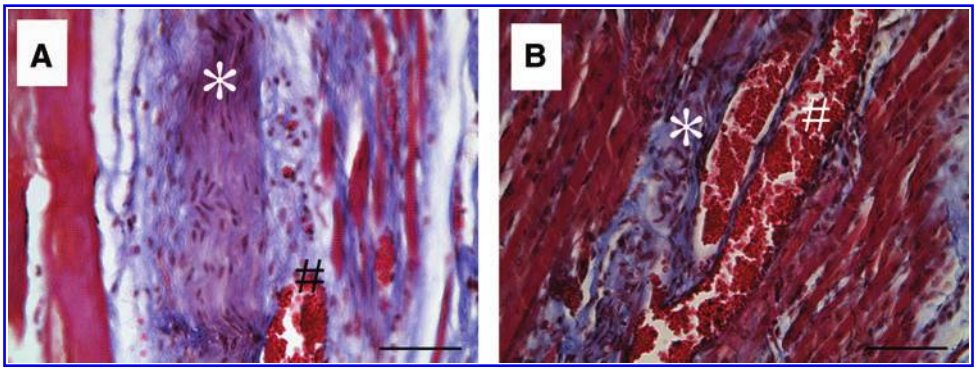

FIG. 5. Presence of vascular and neural structures 1 month after TEMR construct treatment of VML-injured LD muscle. **(A,B)** Images are representative of vascular (#) and neural (*) structures that were identified via characteristic morphology and were observed in all TEMR construct groups 1 month postinjury. Images are 400× magnification; Scale bar = 50 μm. Color images available online at www.liebertonline.com/tea

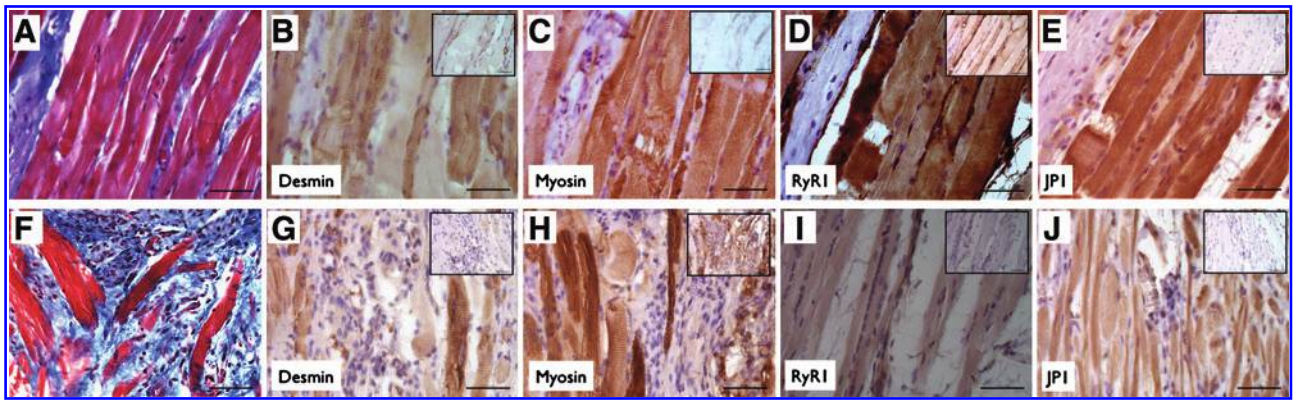

FIG. 6. Functional protein expression in regenerating muscle fibers and putative neo-tissue 2 months after TEMR construct treatment of VML-injured LD muscle. Masson's trichrome staining and immunohistochemical staining for functional proteins is illustrated at the interface between the remaining native tissue and the TEMR construct **[(A–E)**; representative of all TEMR repaired muscle] and for independent tissue formed in BAM scaffolding [**(F–J)**; images derived from TEMR-1SPD and −2SPD-repaired muscle]. Insets show negative control staining for the primary antibody. Images are 400× magnification with the scale bar = 50 μm. Color images available online at www.liebertonline.com/tea

often appear smaller in diameter, suggesting that the regenerative response is not completed in this area (Fig. 6G–J). To determine whether TEMR constructs promoted a prolonged regenerative response, Pax7 protein expression was measured 2 months postinjury (Fig. 7). Pax7 was chosen as a regenerative marker because it is crucial for skeletal muscle regeneration.[41,42] In comparison to uninjured values, Pax7 expression was significantly elevated for all TEMR construct groups, but not for the NR group (Fig. 7).

Discussion

In response to a variety of injuries, skeletal muscle undergoes a well-characterized degenerative and regenerative response aimed at restoring functional capacity to the injured tissue. In fact, most muscle injury models in otherwise healthy young adult rodents report full functional recovery via endogenous regeneration and repair mechanisms.[43–45] In contrast, with VML injury, by definition, the tissue loss is so great that the regenerative capacity of the remaining skeletal muscle tissue is not adequate to restore muscle mass and function in either humans[6,8] or rodents,[12,13] presumably due to the loss of ECM and concomitant depletion of the resident satellite cell population.

As a first step toward development of therapeutics to treat VML injuries, we previously developed an *in vitro* bioreactor-based skeletal muscle tissue engineering model,[12,29] in which MDCs are seeded on acellular collagen scaffolds and are promoted to differentiate and align under chemical and mechanical cues (i.e., TEMR-1SPD in the current study). Implantation of differentiated TEMR constructs significantly restored functional capacity to VML-injured LD muscle 2 months postinjury.[12] Notably, implantation of a BAM, without the inclusion of differentiated MDCs did not improve function at this time,[12] signifying the importance of providing a cellular component for functional restoration of VML injury using this *in vitro* tissue engineering approach and the murine VML injury model employed in the current study.

The primary hypothesis and novelty of the current study is that altering the *in vitro* cellular phenotype and composition of the implanted TEMR construct, prior to implantation *in vivo*, can modulate both the time course and magnitude of functional recovery from VML injury. To this end, we modified our bioreactor-based *in vitro* tissue engineering protocol to produce three distinct TEMR constructs marked by prominent differences in their morphological appearance as follows: (1) randomly organized unfused MDCs (TEMR-1SP), with few, if any, detectable multinucleated myotubes, (2) moderate density of elongated aligned myotubes (approximately two multinucleated myotubes/HPF), interspersed with MDCs (TEMR-1SPD), and (3) relatively dense elongated aligned myotubes (approximately six multinucleated myotubes/HPF), with intervening MDCs (TEMR-2SPD; Fig. 2). Notably, the generation of TEMR-2SPD constructs involved the development of a novel seeding strategy, in which a second application of MDCs to an underlying layer of myotubes was performed during bioreactor preconditioning. This cell seeding strategy increased the number of multinucleated cells comprising TEMR-2SPD constructs, indicating that a portion of the second population of MDCs fused with the underlying differentiated layer—a process observed during embryonic development and adult muscle fiber repair, regeneration, and growth in response to injury and exercise.[22–28] Moreover, while TEMR-2SPD constructs exhibited a differentiated morphological appearance, the muscle protein expression profile was more akin to TEMR-1SP constructs (Fig. 2). Thus, TEMR-2SPD constructs appear to be comprised of cell populations represented in constructs derived under both proliferating (TEMR-1SP) and differentiating (TEMR-1SPD) cell culture and bioreactor protocols. As such, this hybrid construct may impart unique therapeutic benefits that combine the salient characteristics of the other two constructs.

More specifically, TEMR-2SPD constructs promoted a rapid and prolonged functional recovery. The accelerated time course of the functional recovery was analogous to that produced by the TEMR-1SP construct, while the increased and prolonged functional recovery was similar to that produced by the TEMR-1SPD construct. Consistent with a previous study,[12] implantation of TEMR-1SPD constructs was not associated with significant functional recovery, relative

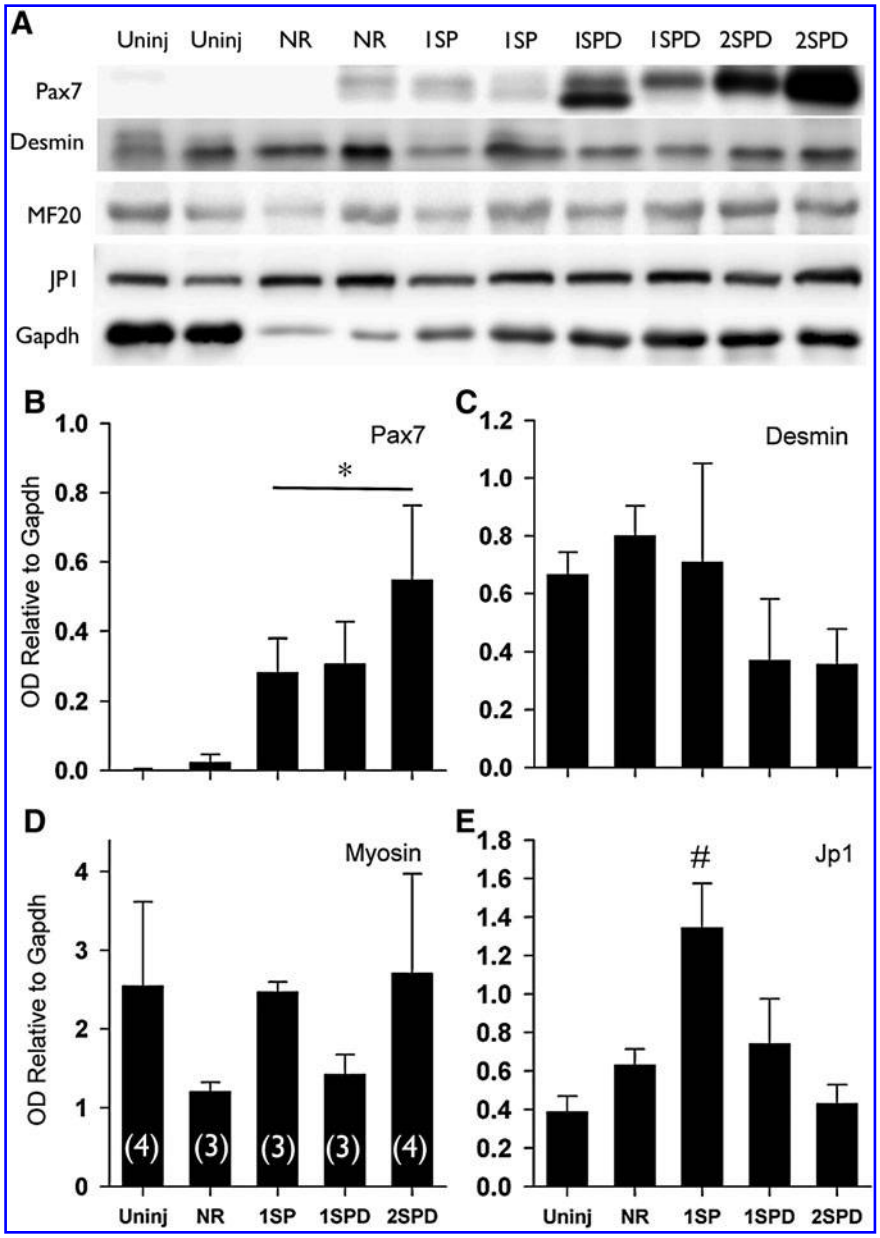

FIG. 7. LD muscle protein expression 2 months postinjury. **(A)** LD muscles were probed for Pax7, desmin, myosin (MF20), junctophilin 1 (JP1), and GAPDH using sodium dodecyl sulfate polyacrylamide gel electrophoresis and Western blotting. **(B–E)** Optical density was determined for each band and normalized to GAPDH. *Significantly different from uninjured; #Significantly different from all other groups ($p < 0.05$). Values are expressed as mean ± SE. Sample sizes for each group are listed in parentheses in panel D.

to unrepaired muscle, until 2 months postinjury (Fig. 3). However, implantation of both TEMR-1SP and TEMR-2SPD constructs was associated with functional restoration at 1 month postinjury. Interestingly, while functional recovery continued to improve from 1 to 2 months postinjury for the TEMR-2SPD group (i.e., to ~70% of uninjured muscle), no such time dependent functional recovery was observed for the TEMR-1SP construct (Fig. 3; Table 1). These data are consistent with the supposition that on the one hand the presence of a significant population of undifferentiated MDCs is important to accelerated functional recovery (the increased recovery observed at the 1 month time point for the TEMR-1SP and TEMR-2SPD constructs), while on the other, the presence of multinucleated myotubes is critical to continuous and sustained functional recovery (i.e., the further increase in contractility observed for the TEMR-1SPD and TEMR-2SPD constructs) in this murine VML injury model.

Although we do not yet know the definitive cellular and molecular mechanisms responsible for these disparate rates of functional recovery among the three TEMR construct types, it is remarkable to note that for LD muscles repaired with TEMR-1SP constructs, at both 1 and 2 months post-implantation, the BAM scaffolding was largely devoid of any cellular presence, while the interface of the BAM and remaining tissue exhibited significant signs of repair and regeneration (Fig. 4). These findings appear to be in line with previous myocardial injury studies in which functional improvement is often associated with poor myoblast engraftment,[46] indicating that potentially angiogenic, neurogenic, or growth and trophic factors primarily mediate myoblast-induced functional recovery in this construct group.[47–49] Likewise, it is possible that TEMR constructs differentiated via bioreactor preconditioning mediate functional recovery via trophic mechanisms as well, however, it is also clear that regenerating muscle fibers are formed independent from

the native tissue in these constructs (Figs. 4 and 6), suggesting that these constructs also directly contribute to neo-muscle fiber formation. In other VML injury models using tissue engineering technologies based primarily on the development of neo-tissue formation (i.e., in the absence of cells), functional recovery often requires extended periods of time until an apparent critical mass of tissue regenerates.[17,18] Thus, it is plausible that differentiated TEMR constructs (i.e., 1SPD and 2SPD) require a relatively shorter regenerative period to promote functional recovery via neo-tissue formation.

Consistent with our previous observations,[12] for the more differentiated TEMR construct types (i.e., TEMR-1SPD and TEMR-2SPD) the functional improvements following implantation appear, at least in part, the result of muscle fiber regeneration (e.g., at the interface or independently within the implanted construct) and not entirely the result of TEMR-mediated hypertrophy of the remaining native tissue. While the observed physiological improvements in absolute isometric and caffeine contracture forces cannot distinguish between these two mechanisms, the presence of regenerating muscle fibers at the interface and within the BAM scaffold with TEMR construct implantation (Figs. 4 and 6) points toward TEMR-mediated regeneration as an important component of functional recovery. In support of this supposition is the fact that if significant fiber hypertrophy of the remaining skeletal muscle tissue occurs, then an increased relative expression of myosin is expected.[50] The fact that the relative muscle protein expression was similar among TEMR-treated muscle and uninjured LD muscle (Fig. 7) suggests that regenerated muscle fibers with a similar protein stoichiometry of uninjured LD muscle is contributing to functional recovery. Lastly, to demonstrate that TEMR construct-mediated regenerating muscle fibers can directly contribute to functional recovery, we documented that regenerating muscle fibers located at the interface of the TEMR construct and the native tissue, and independent of the interface, expresses force-producing (myosin), force-transmitting (desmin), and excitation–contraction coupling proteins (RyR1 and Jp1)[51,52] in a striated manner similar to native muscle (Fig. 6). Taken together with the tissue morphology and neural and vascular components observed in TEMR constructs (Figs. 4 and 5), these data provide compelling evidence for a direct contribution (i.e., contraction) of the TEMR construct-mediated muscle fiber regeneration to the enhanced functional recovery of VML-injured muscle.

Improvements in specific force following tissue engineering treatments of VML-injured muscle have been reported previously.[12,13,18] Although absolute forces were significantly improved compared to NR muscle (Fig. 3; Table 1) in the current study, specific forces were not improved with TEMR construct implantation. This finding is at variance with our previous report that specific force was improved with TEMR construct repair 2 months postinjury,[12] despite the fact that the magnitude of absolute forces were similar between comparable TEMR construct groups in each study (e.g., TEMR-1SPD 2 months postinjury, Machingal *et al.*[12] vs. Current Study: P_o; 222.5 ± 21.7 vs. 200.1 ± 16.3 mN). The persistent specific force deficit with TEMR implantation observed in the current study is likely due to an increased presence of passive elements (i.e., continued presence of BAM scaffold), as this would contribute to an increase in muscle wet weight but not active force. In support, TEMR construct wet weight is ~55 mg prior to implantation (i.e., ~50% of contralateral uninjured LD muscle wet weight) and Masson's trichrome staining indicates that a significant portion of BAM scaffold is remaining 2 months postinjury. In this scenario, the additional BAM wet weight contributes to the consistent increase in LD muscle wet weight for TEMR construct groups (Table 1), and therefore reflects that specific force is grossly underestimated for these repaired muscles. In our previous study, we reported a decrease of TEMR construct-repaired muscle wet weight at 2 months postinjury.[12] We cannot offer a specific reason for this discrepancy between the current and previous studies. Nevertheless, it is important to note that therapeutically, while it is ideal for regenerating muscle to approximate native specific force, indicating that the engineered muscle is of similar contractile quality to the tissue initially lost, the regenerating muscle's absolute force-producing capacity primarily determines the ability to perform occupational tasks. To this point, the TEMR-2SPD construct, which was generated using a novel cell seeding-bioreactor preconditioning technique prior to implantation, produced a nearly threefold increase in absolute force relative to the 1-month unrepaired animal (Table 2). Moreover, the current threefold increase in absolute force (P_o) 2 months postimplantation, is significantly greater than the previously reported twofold increase,[12] and the twofold increases observed in the current report with the TEMR-1SP and TEMR-1SPD constructs 2 months postinjury.

From a mechanistic viewpoint, a variety of cell types including mesenchymal stem cells and quiescient satellite cells have been used previously to restore function to VML-injured muscle.[13,16] The MDCs used in this study were isolated using a method similar to that reported for the isolation of cells from war traumatized muscle,[53] although both adherent and initially nonadherent cells (e.g., satellite cells) were kept in the current study. The MDCs in the current study represent a mixed population of culture-expanded cells and therefore may include satellite cells (myoblasts), fibroblasts, mesenchymal stem cells, and muscle derived stem cells, among other cell types.[12,53,54] The yield of muscle progenitor cells (Pax7+, MyoD+, or desmin+ cells ≈30% of cells; Fig. 1) prior to seeding on BAM is similar to that observed after three preplating stages.[54] However, it is possible that BAM promotes a preferential expansion of myogenic cells, owing to a close approximation of native muscle mechanical properties[55,56] of processed BAM (Fig. 1[38]). In support of this supposition, we have previously observed qualitatively uniform staining for myogenic cells on BAM scaffolding after 3 days of culture.[12] Regardless, TEMR constructs generated with this mixed population of MDCs promoted significant functional recovery and tissue regeneration in murine VML-injured muscle. It remains to be determined whether or not a pure population of MDCs (e.g., satellite cells) would improve these therapeutic outcomes. As such, it is conceivable that the inclusion of fibroblasts, among other cell populations, with myogenic cells in our initial culture is likely to be beneficial for muscle regeneration and functional outcomes, as has been reported previously.[57,58]

Expression of Pax7, a satellite cell marker, has been shown to increase following muscle injury and is crucial for the regeneration of skeletal muscle thereafter.[41,42] In this study, Pax7 expression at the protein level was significantly

elevated in VML-injured LD muscle treated with TEMR constructs 2 months postinjury (Fig. 7). It is interesting to speculate that the increased Pax7 expression 2 months postinjury is the result of an increase in "satellite" cells induced by the presence of the TEMR constructs in general, and in particular, for the TEMR-2SPD constructs (Fig. 7). To this end, cyclic mechanical strain has been shown to inhibit differentiation of satellite cells and myoblasts[59–61] but promotes increased protein synthesis and expression of more mature muscle markers in myotubes.[62–64] Thus, it is possible that the double seeding methodology used to generate TEMR-2SPD constructs results in implantation of a construct that includes and/or better recruits a subpopulation of cells that resemble satellite cells.

In summary, we have demonstrated that TEMR constructs with distinctly different cellular morphologies promote functional recovery of VML-injured muscle at different rates and magnitudes. Importantly, this study describes the development of a novel skeletal muscle bioreactor cell seeding strategy that mimics aspects of "exercise" *in vitro* and produces TEMR constructs that appear to possess intrinsic regenerative qualities of both "proliferating" and "differentiating" TEMR constructs. That is, this novel TEMR construct (TEMR-2SPD) promoted not only a rapid (like TEMR-1SP) but also a prolonged (like TEMR-1SPD) functional recovery in an additive manner, whereby TEMR-1SP and TEMR-1SPD construct-repaired muscle produced twofold greater force and TEMR-2SPD produced threefold greater force than nonrepaired VML-injured muscle. Additionally, we determined that TEMR-mediated regeneration of skeletal muscle fibers results in expression of key functional proteins in a striated appearance and that whole LD muscles repaired with the TEMR-1SPD and TEMR-2SPD constructs express muscle specific proteins, at the interface and within the regenerating BAM scaffold, with relative stoichiometry similar to uninjured LD muscle. These latter findings are important not only because they indicate that TEMR construct treatment mediates regeneration of functional muscle fibers, but also because native-like protein expression following regeneration adds support to the potential safety and efficacy of TEMR constructs as a treatment of human neuromuscular injuries.

Acknowledgments

We would like to thank Dr. Walters and Dr. Rathbone for their critical review of this article and Mrs. Cathy Mathis for her technical assistance with histological procedures. This work was support in part by TATRC DOD grant W81XWH-09-1-0578.

Disclosure Statement

No competing financial interests exist.

References

1. Carlson, B.M. Regeneration fo the completely excised gastrocnemius muscle in the frog and rat from minced muscle fragments. J Morphol **125,** 447, 1968.
2. Carlson, B.M., and Faulkner, J.A. The regeneration of skeletal muscle fibers following injury: a review. Med Sci Sports Exerc **15,** 187, 1983.
3. Ciciliot, S., and Schiaffino, S. Regeneration of mammalian skeletal muscle. Basic mechanisms and clinical implications. Curr Pharm Des **16,** 906, 2010.
4. Warren, G.L., Summan, M., Gao, X., Chapman, R., Hulderman, T., and Simeonova, P.P. Mechanisms of skeletal muscle injury and repair revealed by gene expression studies in mouse models. J Physiol **582,** 825, 2007.
5. White, T.P., and Devor, S.T. Skeletal muscle regeneration and plasticity of grafts. Exerc Sport Sci Rev **21,** 263, 1993.
6. Grogan, B.F., and Hsu, J.R. Volumetric muscle loss. J Am Acad Orthop Surg **19,** S35, 2011.
7. Lawson, R., and Levin, L.S. Principles of free tissue transfer in orthopaedic practice. J Am Acad Orthop Surg **15,** 290, 2007.
8. Norris, B.L., and Kellam, J.F. Soft-tissue injuries associated with high-energy extremity trauma: principles of management. J Am Acad Orthop Surg **5,** 37, 1997.
9. Mase, V.J., Jr., Hsu, J.R., Wolf, S.E., Wenke, J.C., Baer, D.G., Owens, J., Badylak, S.F., and Walters, T.J. Clinical application of an acellular biologic scaffold for surgical repair of a large, traumatic quadriceps femoris muscle defect. Orthopedics **33,** 511, 2010.
10. Gamba, P.G., Conconi, M.T., Lo Piccolo, R., Zara, G., Spinazzi, R., and Parnigotto, P.P. Experimental abdominal wall defect repaired with acellular matrix. Pediatr Surg Int **18,** 327, 2002.
11. Kin, S., Hagiwara, A., Nakase, Y., Kuriu, Y., Nakashima, S., Yoshikawa, T., Sakakura, C., Otsuji, E., Nakamura, T., and Yamagishi, H. Regeneration of skeletal muscle using *in situ* tissue engineering on an acellular collagen sponge scaffold in a rabbit model. ASAIO J **53,** 506, 2007.
12. Machingal, M.A., Corona, B.T., Walters, T.J., Kesireddy, V., Koval, C.N., Dannahower, A., Zhao, W., Yoo, J.J., and Christ, G.J. A tissue-engineered muscle repair construct for functional restoration of an irrecoverable muscle injury in a murine model. Tissue Eng Part A **17,** 2291, 2011.
13. Merritt, E.K., Cannon, M.V., Hammers, D.W., Le, L.N., Gokhale, R., Sarathy, A., Song, T.J., Tierney, M.T., Suggs, L.J., Walters, T.J., and Farrar, R.P. Repair of traumatic skeletal muscle injury with bone-marrow-derived mesenchymal stem cells seeded on extracellular matrix. Tissue Eng Part A **16,** 2871, 2010.
14. Merritt, E.K., Hammers, D.W., Tierney, M., Suggs, L.J., Walters, T.J., and Farrar, R.P. Functional assessment of skeletal muscle regeneration utilizing homologous extracellular matrix as scaffolding. Tissue Eng Part A **16,** 1395, 2010.
15. Page, R.L., Malcuit, C., Vilner, L., Vojtic, I., Shaw, S., Hedblom, E., Hu, J., Pins, G.D., Rolle, M.W., and Dominko, T. Restoration of skeletal muscle defects with adult human cells delivered on fibrin microthreads. Tissue Eng Part A **17,** 2629, 2011.
16. Rossi, C.A., Flaibani, M., Blaauw, B., Pozzobon, M., Figallo, E., Reggiani, C., Vitiello, L., Elvassore, N., and De Coppi, P. *In vivo* tissue engineering of functional skeletal muscle by freshly isolated satellite cells embedded in a photopolymerizable hydrogel. FASEB J **25,** 2296, 2011.
17. Turner, N.J., Yates, A.J., Jr., Weber, D.J., Qureshi, I.R., Stolz, D.B., Gilbert, T.W., and Badylak, S.F. Xenogeneic extracellular matrix as an inductive scaffold for regeneration of a functioning musculotendinous junction. Tissue Eng Part A **16,** 3309, 2010.
18. Valentin, J.E., Turner, N.J., Gilbert, T.W., and Badylak, S.F. Functional skeletal muscle formation with a biologic scaffold. Biomaterials **31,** 7475, 2010.

19. DiMario, J.X., and Stockdale, F.E. Differences in the developmental fate of cultured and noncultured myoblasts when transplanted into embryonic limbs. Exp Cell Res **216,** 431, 1995.
20. Hall, J.K., Banks, G.B., Chamberlain, J.S., and Olwin, B.B. Prevention of muscle aging by myofiber-associated satellite cell transplantation. Sci Transl Med **2,** 57ra83, 2010.
21. Ikemoto, M., Fukada, S., Uezumi, A., Masuda, S., Miyoshi, H., Yamamoto, H., Wada, M.R., Masubuchi, N., Miyagoe-Suzuki, Y., and Takeda, S. Autologous transplantation of SM/C-2.6(+) satellite cells transduced with micro-dystrophin CS1 cDNA by lentiviral vector into mdx mice. Mol Ther **15,** 2178, 2007.
22. Adams, G.R. Satellite cell proliferation and skeletal muscle hypertrophy. Appl Physiol Nutr Metab **31,** 782, 2006.
23. Barton-Davis, E.R., Shoturma, D.I., and Sweeney, H.L. Contribution of satellite cells to IGF-I induced hypertrophy of skeletal muscle. Acta Physiol Scand **167,** 301, 1999.
24. Capers, C.R. Multinucleation of skeletal muscle *in vitro*. J Biophys Biochem Cytol **7,** 559, 1960.
25. Jansen, K.M., and Pavlath, G.K. Molecular control of mammalian myoblast fusion. Methods Mol Biol **475,** 115, 2008.
26. Konigsberg, I.R., McElvain, N., Tootle, M., and Herrmann, H. The dissociability of deoxyribonucleic acid synthesis from the development of multinuclearity of muscle cells in culture. J Biophys Biochem Cytol **8,** 333, 1960.
27. McCarthy, J.J., Mula, J., Miyazaki, M., Erfani, R., Garrison, K., Farooqui, A.B., Srikuea, R., Lawson, B.A., Grimes, B., Keller, C., Van Zant, G., Campbell, K.S., Esser, K.A., Dupont-Versteegden, E.E., and Peterson, C.A. Effective fiber hypertrophy in satellite cell-depleted skeletal muscle. Development **138,** 3657, 2011.
28. Rathbone, C.R., Wenke, J.C., Warren, G.L., and Armstrong, R.B. Importance of satellite cells in the strength recovery after eccentric contraction-induced muscle injury. Am J Physiol Regul Integr Comp Physiol **285,** R1490, 2003.
29. Moon du, G., Christ, G., Stitzel, J.D., Atala, A., and Yoo, J.J. Cyclic mechanical preconditioning improves engineered muscle contraction. Tissue Eng Part A **14,** 473, 2008.
30. Corona, B.T., Balog, E.M., Doyle, J.A., Rupp, J.C., Luke, R.C., and Ingalls, C.P. Junctophilin damage contributes to early strength deficits and EC coupling failure after eccentric contractions. Am J Physiol Cell Physiol **298,** C365, 2010.
31. Corona, B.T., Rouviere, C., Hamilton, S.L., and Ingalls, C.P. Eccentric contractions do not induce rhabdomyolysis in malignant hyperthermia susceptible mice. J Appl Physiol **105,** 1542, 2008.
32. Ingalls, C.P., Warren, G.L., Williams, J.H., Ward, C.W., and Armstrong, R.B. E-C coupling failure in mouse EDL muscle after *in vivo* eccentric contractions. J Appl Physiol **85,** 58, 1998.
33. Brooks, S.V., and Faulkner, J.A. Contractile properties of skeletal muscles from young, adult and aged mice. J Physiol **404,** 71, 1988.
34. Mendez, J., and Keys, A. Density and composition of mammalian muscle. Metabolism **9,** 184, 1960.
35. Sacks, R.D., and Roy, R.R. Architecture of the hind limb muscles of cats: functional significance. J Morphol **173,** 185, 1982.
36. Corona, B.T., Rouviere, C., Hamilton, S.L., and Ingalls, C.P. FKBP12 deficiency reduces strength deficits after eccentric contraction-induced muscle injury. J Appl Physiol **105,** 527, 2008.
37. Shah, A.J., Pagala, M.K., Subramani, V., Venkatachari, S.A., and Sahgal, V. Effect of fiber types, fascicle size and halothane on caffeine contractures in rat muscles. J Neurol Sci **88,** 247, 1988.
38. Feng, C., Xu, Y.M., Fu, Q., Zhu, W.D., Cui, L., and Chen, J. Evaluation of the biocompatibility and mechanical properties of naturally derived and synthetic scaffolds for urethral reconstruction. J Biomed Mater Res A **94,** 317, 2010.
39. Lehti, T.M., Kalliokoski, R., and Komulainen, J. Repeated bout effect on the cytoskeletal proteins titin, desmin, and dystrophin in rat skeletal muscle. J Muscle Res Cell Motil **28,** 39, 2007.
40. Lieber, R.L., Thornell, L.E., and Friden, J. Muscle cytoskeletal disruption occurs within the first 15 min of cyclic eccentric contraction. J Appl Physiol **80,** 278, 1996.
41. Lepper, C., Partridge, T.A., and Fan, C.M. An absolute requirement for Pax7-positive satellite cells in acute injury-induced skeletal muscle regeneration. Development **138,** 3639, 2011.
42. Sambasivan, R., Yao, R., Kissenpfennig, A., Van Wittenberghe, L., Paldi, A., Gayraud-Morel, B., Guenou, H., Malissen, B., Tajbakhsh, S., and Galy, A. Pax7-expressing satellite cells are indispensable for adult skeletal muscle regeneration. Development **138,** 3647, 2011.
43. Ingalls, C.P., Warren, G.L., and Armstrong, R.B. Dissociation of force production from MHC and actin contents in muscles injured by eccentric contractions. J Muscle Res Cell Motil **19,** 215, 1998.
44. Plant, D.R., Beitzel, F., and Lynch, G.S. Length–tension relationships are altered in regenerating muscles of the rat after bupivacaine injection. J Appl Physiol **98,** 1998, 2005.
45. Warren, G.L., Hulderman, T., Mishra, D., Gao, X., Millecchia, L., O'Farrell, L., Kuziel, W.A., and Simeonova, P.P. Chemokine receptor CCR2 involvement in skeletal muscle regeneration. FASEB J **19,** 413, 2005.
46. Formigli, L., Zecchi-Orlandini, S., Meacci, E., and Bani, D. Skeletal myoblasts for heart regeneration and repair: state of the art and perspectives on the mechanisms for functional cardiac benefits. Curr Pharm Des **16,** 915, 2010.
47. Perez-Ilzarbe, M., Agbulut, O., Pelacho, B., Ciorba, C., San Jose-Eneriz, E., Desnos, M., Hagege, A.A., Aranda, P., Andreu, E.J., Menasche, P., and Prosper, F. Characterization of the paracrine effects of human skeletal myoblasts transplanted in infarcted myocardium. Eur J Heart Fail **10,** 1065, 2008.
48. Rhoads, R.P., Johnson, R.M., Rathbone, C.R., Liu, X., Temm-Grove, C., Sheehan, S.M., Hoying, J.B., and Allen, R.E. Satellite cell-mediated angiogenesis *in vitro* coincides with a functional hypoxia-inducible factor pathway. Am J Physiol Cell Physiol **296,** C1321, 2009.
49. Tatsumi, R., Sankoda, Y., Anderson, J.E., Sato, Y., Mizunoya, W., Shimizu, N., Suzuki, T., Yamada, M., Rhoads, R.P., Jr., Ikeuchi, Y., and Allen, R.E. Possible implication of satellite cells in regenerative motoneuritogenesis: HGF upregulates neural chemorepellent Sema3A during myogenic differentiation. Am J Physiol Cell Physiol **297,** C238, 2009.
50. Tsika, R.W., Herrick, R.E., and Baldwin, K.M. Time course adaptations in rat skeletal muscle isomyosins during compensatory growth and regression. J Appl Physiol **63,** 2111, 1987.
51. Balog, E.M. Excitation-contraction coupling and minor triadic proteins in low-frequency fatigue. Exerc Sport Sci Rev **38,** 135, 2010.
52. Lanner, J.T., Georgiou, D.K., Joshi, A.D., and Hamilton, S.L. Ryanodine receptors: structure, expression, molecular

details, and function in calcium release. Cold Spring Harb Perspect Biol **2,** a003996, 2010.
53. Nesti, L.J., Jackson, W.M., Shanti, R.M., Koehler, S.M., Aragon, A.B., Bailey, J.R., Sracic, M.K., Freedman, B.A., Giuliani, J.R., and Tuan, R.S. Differentiation potential of multipotent progenitor cells derived from war-traumatized muscle tissue. J Bone Joint Surg Am **90,** 2390, 2008.
54. Jankowski, R.J., Haluszczak, C., Trucco, M., and Huard, J. Flow cytometric characterization of myogenic cell populations obtained via the preplate technique: potential for rapid isolation of muscle-derived stem cells. Hum Gene Ther **12**, 619, 2001.
55. Helber, R. Elastic and inelastic behaviour of resting frog muscle fibres. Pflugers Arch **387,** 261, 1980.
56. Moss, R.L., and Halpern, W. Elastic and viscous properties of resting frog skeletal muscle. Biophys J **17,** 213, 1977.
57. Brady, M.A., Lewis, M.P., and Mudera, V. Synergy between myogenic and non-myogenic cells in a 3D tissue-engineered craniofacial skeletal muscle construct. J Tissue Eng Regen Med **2,** 408, 2008.
58. Murphy, M.M., Lawson, J.A., Mathew, S.J., Hutcheson, D.A., and Kardon, G. Satellite cells, connective tissue fibroblasts and their interactions are crucial for muscle regeneration. Development **138,** 3625, 2011.
59. Boonen, K.J., Langelaan, M.L., Polak, R.B., van der Schaft, D.W., Baaijens, F.P., and Post, M.J. Effects of a combined mechanical stimulation protocol: value for skeletal muscle tissue engineering. J Biomech **43,** 1514, 2010.
60. Kook, S.H., Lee, H.J., Chung, W.T., Hwang, I.H., Lee, S.A., Kim, B.S., and Lee, J.C. Cyclic mechanical stretch stimulates the proliferation of C2C12 myoblasts and inhibits their differentiation via prolonged activation of p38 MAPK. Mol Cells **25,** 479, 2008.
61. Kook, S.H., Son, Y.O., Choi, K.C., Lee, H.J., Chung, W.T., Hwang, I.H., and Lee, J.C. Cyclic mechanical stress suppresses myogenic differentiation of adult bovine satellite cells through activation of extracellular signal-regulated kinase. Mol Cell Biochem **309,** 133, 2008.
62. Candiani, G., Riboldi, S.A., Sadr, N., Lorenzoni, S., Neuenschwander, P., Montevecchi, F.M., and Mantero, S. Cyclic mechanical stimulation favors myosin heavy chain accumulation in engineered skeletal muscle constructs. J Appl Biomater Biomech **8,** 68, 2010.
63. Hornberger, T.A., Armstrong, D.D., Koh, T.J., Burkholder, T.J., and Esser, K.A. Intracellular signaling specificity in response to uniaxial vs. multiaxial stretch: implications for mechanotransduction. Am J Physiol Cell Physiol **288,** C185, 2005.
64. Vandenburgh, H.H., Hatfaludy, S., Karlisch, P., and Shansky, J. Skeletal muscle growth is stimulated by intermittent stretch-relaxation in tissue culture. Am J Physiol **256,** C674, 1989.

Author correspondence to:
George J. Christ, Ph.D.
Wake Forest Institute for Regenerative Medicine
Wake Forest University Baptist Medical Center
Richard H. Dean Biomedical Research Building, Room 257
391 Technology Way
Winston-Salem, NC 27101

E-mail: gchrist@wakehealth.edu

Received: October 30, 2011
Accepted: January 27, 2012
Online Publication Date: May 10, 2012

This article has been cited by:

1. Tracy L. Criswell, Benjamin T. Corona, Zhan Wang, Yu Zhou, Guoguang Niu, Yong Xu, George J. Christ, Shay Soker. 2013. The role of endothelial cells in myofiber differentiation and the vascularization and innervation of bioengineered muscle tissue in##vivo. *Biomaterials* **34**:1, 140-149. [CrossRef]
2. Xiaowu Wu , Benjamin T. Corona , Xiaoyu Chen , Thomas J. Walters . 2012. A Standardized Rat Model of Volumetric Muscle Loss Injury for the Development of Tissue Engineering Therapies. *BioResearch Open Access* **1**:6, 280-290. [Abstract] [Full Text HTML] [Full Text PDF] [Full Text PDF with Links] [Supplemental Material]